

Hydrodynamic modes in a trapped gas of metastable helium above the Bose-Einstein transition

M. Leduc, J. Léonard, F. Pereira dos Santos, E. Jahier, S. Schwartz and C. Cohen-Tannoudji
*Collège de France et Laboratoire Kastler Brossel,
 Département de Physique, École Normale Supérieure,
 24 rue Lhomond, 75231 Paris Cedex 05, France*
 (October 23, 2018)

This article describes experiments performed with an ultracold gas of metastable helium above the Bose-Einstein transition. The gas is trapped in an harmonic magnetic potential and collective excitations are induced. Both the frequency and the damping rate of the lowest monopole-quadrupole $m = 0$ mode of excitation are studied at different temperatures and compared to theoretical predictions. Results indicate that the gas goes from a collisionless regime towards a hydrodynamic regime as the elastic collision rate increases, when one goes down along the evaporative cooling ramp. However we find a discrepancy for the collisional parameters in comparison with predictions relying on the value of the scattering length previously estimated. Possible explanations are put forward in the final discussion.

I. INTRODUCTION

Soon after the experimental realization of Bose-Einstein condensation in trapped atomic gases, studies of collective excitations in these systems have become a subject of intense investigation by several groups [1–6]. At very low temperature, when the system is Bose-Einstein condensed, it can be described by the hydrodynamic equations of a superfluid [4,7], which give predictions in good agreement with experiments performed with alkali condensates. At higher temperature, the mean field effects become less important and collisions turn out to be the dominant factors. For an ultracold gas above the critical temperature of condensation, the dynamical behavior of the dilute gas can be described by the Boltzmann equation. In this case two extreme situations can occur: - the hydrodynamic regime, where the mean free path between the colliding particles is small compared to the dimensions of the cold cloud confined in its trap - and the collisionless regime where the motion is described by the single particle Hamiltonian. In both cases, when excited, the system shows well-defined oscillations resulting from the external magnetic confinement, for which predictions have been made (see for instance [5] or [6] and references therein). The frequency and the damping rates of the gas oscillations can be calculated for a classical gas confined in an harmonic trap, neglecting the mean field effects. In reference [6] results are given for the monopole-quadrupole modes of excitation, both for the hydrodynamic and for the collisionless regime, with an explicit description of the transition between the two regimes. Many experimental studies have focused on collective excitations of such gases. Experiments have studied low-lying excitations over large ranges of temperature. For all the available data dealing with the thermal cloud of trapped alkali gases significantly above the crit-

ical temperature T_c the regime is collisionless, due to the relatively low value of the atomic density and of the s -wave scattering length ruling the elastic collision rate at very low temperatures. Experiments performed at MIT with a dense gas of sodium provided oscillations of the thermal cloud analogous to first sound and approaching the hydrodynamic regime [3]. However this regime was never completely reached and the complete check of the predictions of [6] is still to come.

When Bose-Einstein condensation of metastable helium was first achieved in 2001 [8,9], it was soon realized that the large estimated value of the scattering length (16 ± 8 nm) would favor a situation where the hydrodynamic regime could be observed in the thermal cloud above T_c . In particular our experiment at ENS seemed appropriate for such a study because of its relatively large number of atoms at the transition (8×10^6). We thus decided to focus on the study of collective excitations in the thermal cloud above T_c . The present article first briefly recalls the experimental set-up and the quantitative results already obtained for the relevant parameters: atomic density, temperature, elastic collision rate at the end of the evaporative cooling ramp. Then we explain the generation of excitations in the cigar shaped thermal cloud and describe the optical measurements of the oscillations of the monopole-quadrupole $m = 0$ mode generated along the weak axis of the cloud. The data for the damping and the frequency of the mode are compared with the predictions of reference [6] and a discussion follows. In particular one finds a discrepancy between the elastic collision rate estimated from the initial data of [9] and those actually measured through the present method.

II. MAGNETIC TRAPPING AND OPTICAL DETECTION

The production of a Bose-Einstein condensate of ^4He atoms in the metastable 2^3S_1 state at ENS is first reported in [9] and described in more detail in [10]. The metastable atoms are produced from a cryogenic discharge source at a rate of 10^{14} at/s/sr. The atomic beam is manipulated by a laser operating on the $2^3S_1 - 2^3P_2$ transition of the helium atom at $1.083\text{ }\mu\text{m}$. After transverse collimation, deflection and longitudinal deceleration in a 2 m long Zeeman slower, the beam loads a magneto-optical trap using laser beams with a large detuning compensated by a large intensity, in order to minimise the rate of inelastic Penning collisions induced by the laser [11–16].

The atomic cloud of typically 10^9 atoms at 1 mK is then transferred into a magnetic trap through a multistep process [10] with an efficiency of about 75%. The magnetic trap that we use for the confinement is sketched in figure 1.

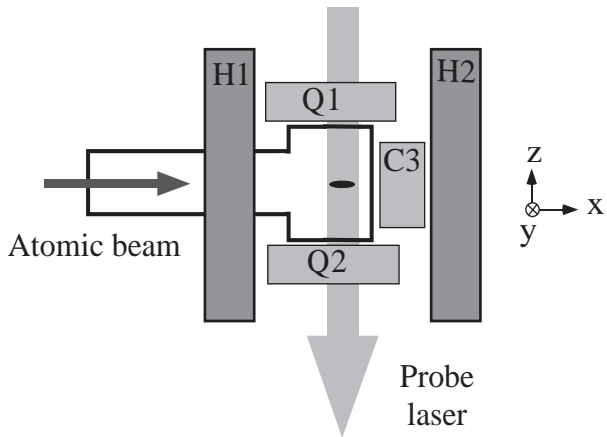


FIG. 1. Magnetostatic trap for the harmonic confinement of the cold helium gas. Q1, Q2, C3 are the Ioffe-Pritchard coils, H1 and H2 are the Helmholtz coils for the bias compression. The detection is optical, using the absorption of a probe laser beam imaged on a CCD camera.

Three coils Q1, Q2, C3 of relatively small size realize an anisotropic magnetic Ioffe-Pritchard trap. Two additional Helmholtz coils H1 and H2 reduce the bias field in order to increase the radial confinement. A current of 46.6 A in all five coils produces a 5 G bias field, radial gradients of 266 G/cm and an axial curvature of 186 G/cm². The trap depth is then about 16 mK, the trap frequency along the x axis (\parallel) is $\omega_{\parallel}/2\pi = \omega_x/2\pi = 115\text{ Hz}$. The radial frequency is $\omega_y/2\pi = \omega_z/2\pi = 190\text{ Hz}$ without compensation of the bias and 988 Hz with a 5 G bias field. The cold cloud at thermal equilibrium has a cigar shape, elongated along the x axis and with a cylindrical symmetry in the radial directions along the y and z axis. When required the cloud can be further compressed in the radial

direction: for this we use another pair of Helmholtz coils delivering an additional field along the x axis which reduces the value of the bias field below 5 G down to nearly 0. The current in the 5 coils can be switched off in 200 μs , but eddy currents induced in several pieces of the set-up in the vicinity of the cell create relatively strong transient field gradients which disappear with a time scale of a few ms. One has to take into account this phenomenon which can create some difficulties when deducing quantitative values from time of flight measurements.

The optical detection is shown in Fig. 1. One measures the absorption of a laser probe beam passing through the atomic cloud with a CCD camera (Hamamatsu C4880) with 1.5% efficiency at the wavelength $\lambda = 1.083\text{ }\mu\text{m}$. The laser source is a DBR diode laser (SDL 60702 H1) operated in an extended cavity and amplified by an Yb doped amplifier. The probe pulse is long enough (100 μs) and intense enough ($I = 0.2I_{sat}$) to give a reasonable signal to noise ratio in spite of the low efficiency of the detector. The magnification being of the order of 1, the resolution of the images is given by the size of the detector pixel, namely 24 μm . Usually the image of the cold cloud in the trap is too small to be detected with a good resolution. Thus after switching off the trap, we let the cloud expand for a few ms and take a picture. We deduce from the images both the actual size of the cloud in the trap and its temperature.

The temperature is ramped down in the magnetic trap by evaporative cooling. Details about the optimisation of the ramp are given in reference [10]. In 8 s one decreases the temperature down to the μK range, whereas the phase space density increases by 6 orders of magnitude and one reaches the Bose-Einstein condensation around 5 μK . At the threshold of the transition the dimensions of the cloud have decreased to 90 and 9 μm in the axial and radial directions, respectively.

III. RELEVANT PARAMETERS

A. Number of atoms

An important parameter for collision studies is the total number of atoms. As already discussed in [9], a proper calibration of this number N is difficult to extract with a good precision from the absorption images, due to various difficulties dealing with the duration of the pulse, the Penning collisions that it induces, its pushing of the atoms, and stray magnetic fields produced by eddy currents. We are currently developing a calibration method based on fluorescence measurements that will be published elsewhere. For the time being we prefer to rely on the method discussed in [9] based on the determination of the critical temperature T_c for the condensation. T_c is deduced from measurements of the relative number of atoms in the condensate and in the thermal cloud as a

function of temperature. The determination of the critical temperature does not require knowing the absolute number of atoms in each phase. However it can be used to evaluate the number of atoms N_c at the transition, assuming that one deals with an ideal bosonic gas. If so, N_c and T_c are related by:

$$N_c = 1.2(k_b T_c / h \bar{\nu})^3 \quad (1)$$

where h is the Planck constant, k_b the Boltzmann constant and $\bar{\nu}$ the geometrical average of frequencies of the trap (482 Hz). Measurements of reference [9] gave $T_c = 4.7 \pm 0.5 \mu\text{K}$. One thus deduces $N_c = 8.2 \times 10^6$ atoms with an uncertainty of 30%. We neglected the possible errors resulting either from mean field interactions or from quantum correlations (see the discussion of note 13 in reference [9]). Once calibrated at T_c the number of atoms N is deduced for any temperature above T_c .

B. Scattering length

The scattering length a is another important parameter relevant for the present studies, as the scattering processes for metastable helium atoms occur only in the s -wave channel at very low temperatures. There are several ways of estimating the value of a from the present experiment. All of them suppose that the absolute number of atoms is known. As the uncertainty on this number is large, the value of a is also derived with a large error bar. We here chose to rely on the method described in [9], in which the scattering length is deduced from the size of the condensate. Its value is determined from the characteristic size of the ground state of the trap and from the chemical potential μ , which can be calculated from the size of the condensate in the Thomas-Fermi limit [4]. We then find the value $a = 16 \pm 8 \text{ nm}$, consistent with the experimental measurement of [8] and theoretical calculations of [18] and [19] estimating a of the order of 8 nm (with no error estimate). A recent calculation [20] is also compatible with the present experimental value but does not give more indication on its precision.

C. Elastic collision rates

Finally from the previous values of parameters N_c and a , one can deduce a value for the elastic collision rate Γ_{coll} in the thermal cloud just at the transition before condensation. We use the simple formula:

$$\Gamma_{coll} = \bar{n} \sigma \bar{v} \quad (2)$$

where \bar{n} is the average density and \bar{v} is the mean relative velocity of the atoms at the transition temperature of 4.7

μK . One easily finds that:

$$\bar{v} = 4 \sqrt{\frac{k_b T}{\pi m}} = 23 \text{ cm s}^{-1}$$

and

$$\bar{n} = 1.4 \times 10^{13} \text{ cm}^{-3}.$$

The value of the cross section σ is estimated from that of the scattering length by:

$$\sigma = 8\pi a^2 = 6.4 \times 10^{-11} \text{ cm}^2$$

which finally results in:

$$\Gamma_{coll} = 2 \times 10^4 \text{ s}^{-1}. \quad (3)$$

The uncertainty on this value is estimated within a factor of 4 which combines those on a , on N_c and on T . However it can be compared to the low angular frequency of the trap ($\omega_{\parallel} = 2\pi \times 115 \text{ Hz}$), and one finds a ratio $\omega_{\parallel}/\Gamma_{coll} = 0.04$, much smaller than 1. A collision rate higher than the trap frequency also means that the mean free path $L \sim 1/\bar{n}\sigma$ of the atoms between collisions is smaller than the dimensions of the cloud. Near the critical temperature, $L \sim 11 \mu\text{m}$, which is smaller than the size of the cloud along the weak axis $\sigma_{\parallel} \sim 140 \mu\text{m}$. We can thus assume that one enters into the hydrodynamic regime, an interesting feature for a cold gas above the transition, as stated in the introduction. These results motivated us to undertake the following studies of the collective excitations in the thermal cloud above T_c .

IV. GENERATION AND DETECTION OF EXCITATION MODES

We decided to generate the lowest excitation modes in the cold gas. The goal of this study is to observe the oscillations of the cold cloud in the axial direction after it receives a kick appropriate to generate the monopole-quadrupole $m = 0$ mode. Let us recall that in an anisotropic trap the modes $l = m = 0$ (monopole) and $l = 2, m = 0$ (quadrupole) are coupled and this results in two so-called '*monopole-quadrupole*' modes. We study the low-frequency monopole-quadrupole mode, for which the axial and radial oscillations are in opposite phase.

The calculations of reference [6] predict changes for the frequency ω_Q and for the damping Γ_Q of the oscillation mode when the collision rate varies from a collisionless regime to a hydrodynamic regime (see Fig. 3). We thus decided to measure the response in time of the ellipticity of the cloud after the mode is excited. We repeated the measurements at various temperatures above T_c in a large range of collision rates, expecting to reach the hydrodynamic regime at the vicinity of the condensation transition.

The excitation is made by a transient pulse of magnetic field giving a kick to the trapped cloud. Several procedures were used and finally we found that the most efficient one is the following one:

- One starts with the gas at rest in the trap at a given temperature T above T_c in the conditions used for the evaporative cooling ramp, namely with a bias field B_0 of 5 G resulting of an equal current in the 5 coils of the trap.

- One abruptly lowers the bias field B_0 along the weak axis (x direction) to a fraction of a Gauss by applying an appropriate current to the additional bias coils mentioned above. This creates a compression in the radial direction, the cloud becomes very elongated. The trap is no longer harmonic but the atomic density increases dramatically.

- One simultaneously creates a sinusoidal modulation of this compression field with the additional bias coils. The amplitude of the short modulation pulse is of order 0.15 G, its duration of order 15 ms (3 periods). We chose a modulation frequency of 180 Hz, intermediate between $2\nu_{\parallel}$ and $1.55\nu_{\parallel}$ which are the expected frequencies for the low frequency monopole-quadrupole mode in the two extreme cases, the collisionless regime and the hydrodynamic regime [6].

- Just after this pulse one changes the bias field again and sets it to about 2 G, a value significantly lower than the usual bias field B_0 of 5 G. This value is chosen in order to obtain the maximum compression of the gas compatible with an harmonic trap. On the one hand the higher the compression, the larger the collision rate, facilitating the entrance into the hydrodynamic regime. On the other the trap has to remain harmonic, meaning that the condition $\mu B/k_b T \gg 1$ must remain fulfilled, to avoid that the intrinsic frequency of the trap is changed by the anharmonicity.

One can show that such a procedure allows to excite the low frequency monopole-quadrupole mode $m = 0$.

V. EXPERIMENTAL RESULTS, COMPARISON WITH THEORY

We monitor the evolution of the ellipticity of the cloud as a function of time after the oscillation is produced. Actually the ellipticity oscillates at the same frequency as the collective mode with the same damping in case of a sufficiently small excitation. A measurement is shown in Fig.2.

From such data one extracts the oscillation frequency ω_Q and the damping rate Γ_Q of the excitation mode. For instance the results of Fig. 2, taken at $3T_c$, give $\omega_Q/2\pi = 191 \pm 6$ Hz and $\Gamma_Q/2\pi = 25.3 \pm 0.8$ Hz. This experiment is repeated several times at different values of the elastic collision rate obtained by varying the final frequency of the RF knife of the evaporation ramp.

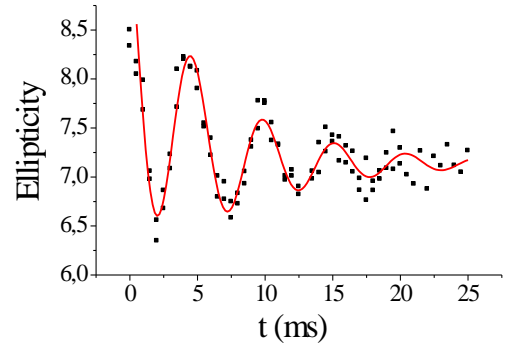


FIG. 2. Oscillations of the ellipticity of the atomic cloud in the monopole-quadrupole $m = 0$ mode. The frequency and damping given by the fit are $\omega_Q/\omega_{\parallel} = 1.66$ and $\Gamma_Q/\omega_{\parallel} = 0.22$.

The results are compared with the predictions of the classical theory of reference [6], which are recalled in Fig. 3.

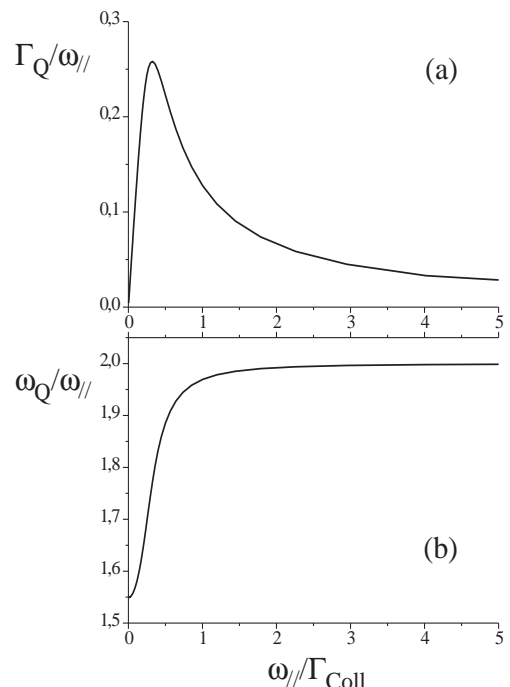


FIG. 3. Theoretical predictions of [6] for the low frequency monopole-quadrupole mode $m = 0$ of an elongated cloud of cold gas as a function of the elastic collision rate. On the upper part (Fig. 3a) is plotted the damping of the oscillations, and on the lower part (Fig. 3b) the frequency of the oscillations, both in units of ω_{\parallel} , the axial (weak) frequency of the trap (Figure taken from [6]).

These results derive both from numerical simulations and from analytical calculations, which are in excellent agreement. One notes that the ratio $\omega_Q/\omega_{\parallel}$ decreases from 2 for the collisionless regime to 1.55 for the hydrodynamic regime, whereas $\Gamma_Q/\omega_{\parallel}$ goes to 0 at both ends but reaches a maximum in between the two regimes. The results of Fig. 3a and Fig. 3b can be combined to give the curve of Fig. 4.

Fig.4 shows the experimental data we obtained. The advantage of such a presentation is that only relative values of the measured frequencies are used, which are known with good precision. One does not require knowledge of the collision rates, which is difficult due to the uncertainties in the present stage of the experiment. In Fig. 4 we plotted the points (called "ENS") corresponding to the highest collision rates that we were able to achieve at a temperature of about $3T_c$. The comparison between experimental data and theoretical calculation allows us to make an indirect measurement of the elastic collision rate in the excited cloud. The highest collision rate that we obtained is in the range of $3.5 \times 10^3 \text{ s}^{-1}$. One remarks that we were unable to reach the expected collision rate of $2 \times 10^4 \text{ s}^{-1}$ which is indicated with a cross in Fig. 4 and which was estimated independently at the transition [9]. We also plotted the results obtained by the group of W. Ketterle at MIT [3] for cold Na atoms.

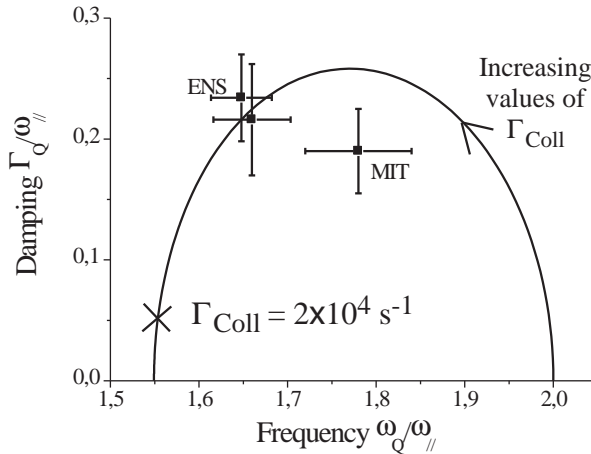


FIG. 4. Plot of the frequencies and damping rates of the lowest monopole-quadrupole mode $m=0$. The solid line summarizes the theoretical calculation already mentioned in Fig.3. The cross corresponds to the estimated value of the collision rate $\Gamma_{coll} = 2 \times 10^4 \text{ s}^{-1}$ for metastable helium as derived from [9]. The arrow indicates the displacement on the curve when Γ_{coll} increases. ENS: Experimental results of this work for metastable helium. MIT: Experimental data point of [3] for sodium.

VI. DISCUSSION

Usually, when the initial elastic collision rate is high enough, the RF evaporation ramp enters in the so-called run-away regime, where both phase space density and Γ_{coll} increase exponentially. So we expect to measure the highest collision rate at the Bose-Einstein transition. In our case, we observed that the phase space density always increases (leading to the Bose-Einstein condensation) but on the contrary, at the very end of the evaporation ramp, the collision rate starts to decrease. The two behaviors are not incompatible since the phase space

density scales like N/T^3 whereas the collision rate scales like N/T . Monitoring the evolution of the elastic collision rate along the evaporation ramp can be easily done while monitoring the optical density (OD) at the center of the cloud. Actually, both quantities are proportional in a harmonic trap : $OD \propto N/T \propto \Gamma_{Coll}$. The evolution of the optical density of the cloud during the evaporative cooling is plotted in Fig. 5. This plot shows that the highest elastic collision rate we can produce is obtained at about $3T_c$. Then, instead of getting deeper into the hydrodynamic regime, the elastic collision rate turns back towards lower values while approaching the transition.

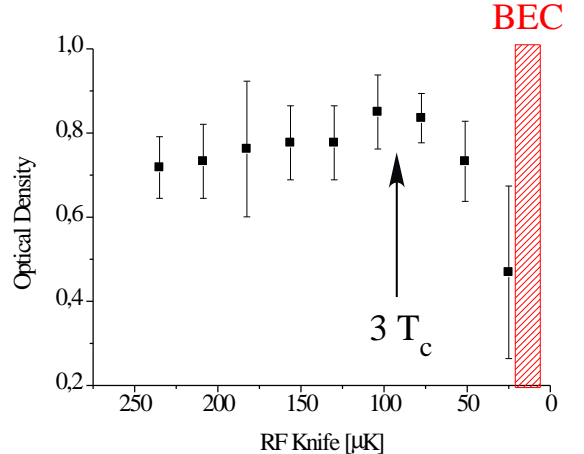


FIG. 5. Measurement of the optical density at the center of the cloud as a function of the trap depth at the end of the evaporative cooling ramp. The optical density being proportional to the elastic collision rate in a harmonic trap, this plot shows that one leaves the run-away regime below a temperature of about $3T_c$.

Actually, while studying the monopole-quadrupole excitation, the highest elastic collision rate measured in Fig. 4 ($\Gamma_{Coll}^{max} \sim 3.5 \times 10^3 \text{ s}^{-1}$) was obtained after evaporation down to about $3T_c$, and *after additional compression* of the magnetic trap. From this value we can infer the corresponding elastic collision rate before additional compression : $2 \times 10^3 \text{ s}^{-1}$. Then, from Fig. 5 we can infer the collision rate at the critical temperature T_c which is about twice as small, leading to 10^3 collisions per second. This value is about 20 times smaller than the one derived from the measurement of the critical temperature of the phase transition.

Within our error bars, assuming 8 nm for the scattering length instead of 16 nm reduces by 4 the discrepancy between the two independent measurements of the elastic collision rate. Then, when we first estimated the collision rate knowing the critical temperature, the number of atoms at the transition was nearly twice as large as it was when we produced collective excitations, which also explains part of the discrepancy. Still it is not enough to conclude to the agreement between the two values. We are still working on improving the accuracy of both kinds

of measurement to understand the discrepancy. In particular we started studying in more detail the effects of eddy currents on the measurement of the temperature. In fact, magnetic fields remaining after the switching off of the trap Zeeman shift the optical lines and modify the absorption cross section of atoms during the optical detection. This modification is not homogeneous in space and might lead to a systematic error on the effective measurement of the size of the cloud after free expansion, and, consequently, of the critical temperature.

In order to find out why we leave the run-away regime at the end of the evaporative ramp, we studied losses and heating rates. For instance we measured heating rates of $20 \mu\text{K/s}$ at $3T_c$. A possible explanation is related to inelastic Penning Ionization taking place when the density becomes high enough. A dominant process is the formation of He^+ ions and He atoms in the ground state which have very large kinetic energy originated from the internal energy of the metastable atoms (about 20 eV). These hot products might collide with trapped metastable atoms and heat them up *via* elastic collisions [21]. Estimates from numbers given in [21] lead to the right order of magnitude for the heating rate. The more hydrodynamic, the more efficient the heating process will be [22], apparently leading to a limitation in the highest elastic collision rate we can produce.

In conclusion, the route towards the hydrodynamic limit has been explored further than in any other reported experiment on collective excitation modes. Especially the measured frequency of the excited mode is strongly shifted towards the hydrodynamic regime as predicted. The experiment is still under progress, and we hope to go deeper into the hydrodynamic regime. However, intrinsic limitations due to inelastic collisions have been found.

Acknowledgements: The authors wish to thank the writers of [6] for allowing the reproduction of part of their work (Fig. 3). This work was supported by La Région Ile-de-France through SESAME contract number 521027.

- [1] S. Giorgini, L. P. Pitaevskii, S. Stringari, *Phys. Rev. Lett.* **78**, 3987 (1997)
- [2] D. S. Jin, M. R. Matthews, J. R. Ensher, C. E. Wieman, and E. A. Cornell, *Phys. Rev. Lett.* **78**, 764 (1997)
- [3] D. M. Stamper-Kurn, H.-J. Miesner, S. Inouye, M. R. Andrews, W. Ketterle, *Phys. Rev. Lett.* **81**, 500 (1998)
- [4] F. Dafolvo, S. Giorgini, L. P. Pitaevskii, S. Stringari, *Rev. Mod. Phys.* **71**, 463 (1999)
- [5] A. Griffin, Wen-Chin Wu, S. Stringari, *Phys. Rev. Lett.* **78**, 1838 (1997)
- [6] D. Guéry-Odelin, F. Zambelli, J. Dalibard, S. Stringari, *Phys. Rev. A* **60**, 4851 (1999)
- [7] S. Stringari, *Phys. Rev. Lett.* **77**, 2360 (1996)
- [8] A. Robert, O. Sirjean, A. Browaeys, J. Poupard, S. Nowak, D. Boiron, C.I. Westbrook, A. Aspect, *Science Mag.* 292, 463 (2001)
- [9] F. Pereira dos Santos, J. Léonard, Junmin Wang, C. J. Barrelet, F. Perales, E. Rasel, C. S. Unnikrishnan, M. Leduc, C. Cohen-Tannoudji, *Phys. Rev. Lett.* **86**, 3459 (2001)
- [10] F. Pereira dos Santos, J. Léonard, Junmin Wang, C. J. Barrelet, F. Perales, E. Rasel, C. S. Unnikrishnan, M. Leduc and C. Cohen-Tannoudji, *Eur. Phys. J. D*, **19**, 103 (2002)
- [11] F. Bardou, O. Emile, J.M. Courty, C.I. Westbrook and A. Aspect, *Europhys. Lett.* **20**, 681 (1992)
- [12] H.C. Mastwijk, J.W. Thomsen, P. van der Straten and A. Niehaus, *Phys. Rev. Lett.* **80**, 5516 (1998).
- [13] M. Kumakura and N. Morita, *Phys. Rev. Lett.* **82**, 2848 (1999).
- [14] P.J.J. Tol, N. Herschbach, E.A. Hessels, W. Hogervorst, W. Vassen, *Phys. Rev. A* **60**, R761 (1999)
- [15] F. Pereira Dos Santos, F. Perales, J. Léonard, A. Sinatra, Junmin Wang, F. S. Pavone, E. Rasel, C. S. Unnikrishnan and M. Leduc, *Eur. Phys. J. D* **14**, 15 (2001)
- [16] A. Browaeys, J. Poupard, A. Robert, S. Nowak, W. Roodijkers, E. Arimondo, L. Marcassa, D. Boiron, C.I. Westbrook and A. Aspect, *Eur. Phys. J. D* **8**, 199 (2000)
- [17] Y. Castin, R. Dum, *Phys. Rev. Lett.* **77**, 5315 (1996)
- [18] P. O. Fedichev, M. W. Reynolds, U. M. Rahmanov, G. V. Shlyapnikov, *Phys. Rev. A* **53**, 1447 (1996)
- [19] V. Venturi, I. B. Whittingham, *Phys. Rev. A* **61**, 060703 (2000)
- [20] F. X. Gadéa, T. Leininger, A. S. Dickinson, to be published in *J. Chem. Phys.*
- [21] H. C. W. Beijerinck, E. J. D. Vredenbregt, R. J. W. Stas, M. R. Doery, and J. G. C. Tempelaars, *Phys. Rev. A* **61** 023607 (2000)
- [22] J. Schuster, A. Marte, S. Amtage, B. Sang, G. Rempe, H. C.W. Beijerinck, *Phys. Rev. Lett.* **87**, 170404 (2001)

- [1] S. Giorgini, L. P. Pitaevskii, S. Stringari, *Phys. Rev. Lett.* **78**, 3987 (1997)
- [2] D. S. Jin, M. R. Matthews, J. R. Ensher, C. E. Wieman, and E. A. Cornell, *Phys. Rev. Lett.* **78**, 764 (1997)
- [3] D. M. Stamper-Kurn, H.-J. Miesner, S. Inouye, M. R. Andrews, W. Ketterle, *Phys. Rev. Lett.* **81**, 500 (1998)
- [4] F. Dafolvo, S. Giorgini, L. P. Pitaevskii, S. Stringari, *Rev. Mod. Phys.* **71**, 463 (1999)
- [5] A. Griffin, Wen-Chin Wu, S. Stringari, *Phys. Rev. Lett.* **78**, 1838 (1997)